

Supplementary Material

for

C–H Activation of Terpyridine-Stereoisomers with Ni(II), Pd(II), and Pt(II)

Leo Payen, Lukas Kletsch, Tobias Lapić, Mathias Wickleder, and Axel Klein*

Universität zu Köln, Department für Chemie, Institut für Anorganische Chemie, Greinstraße 6, D-50939 Köln, Germany; Email: lpayen@smail.uni-koeln.de; ORCID: 0000-0003-1291-9690 (L.P.); Email: lukas.kletsch@uni-koeln.de, ORCID: 0000-0001-9970-6967 (L.K.). Email: tlapic@smail.uni-koeln.de; ORCID: 0000-0003-3115-6756 (T.L.). Email: mathias.wickleder@uni-koeln.de; ORCID: 0000-0002-8864-4227 (M.W.).

* Correspondence: axel.klein@uni-koeln.de (A.K.); ORCID: 0000-0003-0093-9619; Tel.: +49-221-470-4006 (A.K.)

Contents

1. Syntheses

2. Supplementary Figures

Figure S1. Molecular structure of $[\text{Ni}(2,3':5',2''\text{-terpy})\text{Br}_{0.14}/\text{OAc}_{0.86}]\cdot\text{H}_2\text{O}$.

Figure S2. View on the crystal structure of $[\text{Ni}(2,3':5',2''\text{-terpy})\text{Br}_{0.14}/\text{OAc}_{0.86}]\cdot\text{H}_2\text{O}$ along the crystallographic *a*-axis.

Figure S3. View on the crystal structure of $[\text{Ni}(2,3':5',2''\text{-terpy})\text{Br}_{0.14}/\text{acetate}_{0.86}]\cdot\text{H}_2\text{O}$ along the crystallographic *b*-axis.

Figure S4. View on the crystal structure of $[\text{Ni}(2,3':5',2''\text{-terpy})\text{Br}_{0.14}/\text{acetate}_{0.86}]\cdot\text{H}_2\text{O}$ along the crystallographic *c*-axis.

Figure S5. Molecular structure of $[\text{Pd}(2,3':5',2''\text{-terpyH})\text{Cl}_2]$.

Figure S6. View on the crystal structure of $[\text{Pd}(2,3':5',2''\text{-terpyH})\text{Cl}_2]$ along the crystallographic *a*-axis.

Figure S7. View on the crystal structure of $[\text{Pd}(2,3':5',2''\text{-terpyH})\text{Cl}_2]$ along the crystallographic *b*-axis.

Figure S8. View on the crystal structure $[\text{Pd}(2,3':5',2''\text{-terpyH})\text{Cl}_2]$ along the crystallographic *c*-axis.

Figure S9. Molecular structure of $[\text{Pt}(2,3':5',2''\text{-terpyH})\text{Cl}]\text{Cl}$.

Figure S10. View on the crystal structure of $[\text{Pt}(2,3':5',2''\text{-terpyH})\text{Cl}]\text{Cl}$ along the crystallographic *a*-axis.

Figure S11. View on the crystal structure of $[\text{Pt}(2,3':5',2''\text{-terpyH})\text{Cl}]\text{Cl}$ along the crystallographic *b*-axis.

Figure S12. View on the crystal structure of $[\text{Pt}(2,3':5',2''\text{-terpyH})\text{Cl}]\text{Cl}$ along the crystallographic *c*-axis.

Figure S13. Cyclic voltammograms of 2,2':6',3''-terpy and 2,2':6',4''-terpy.

Figure S14. Cyclic voltammograms of 2,3':5',2''-terpy and 2,2':4',2''-terpy.

Figure S15. Cyclic voltammograms of $[\text{Ni}(2,3':5',2''\text{-terpy})\text{Br}]$ and $[\text{Ni}(2,2':4',2''\text{-terpy})\text{Br}]$.

Figure S16. Cyclic voltammograms of $[\text{Pd}(2,3':5',2''\text{-terpy})\text{Cl}]$ and $[\text{Pd}(2,2':4',2''\text{-terpy})\text{Cl}]$.

Figure S17. Cyclic voltammograms of $[\text{Pt}(2,3':5',2''\text{-terpy})\text{Cl}]$ and $[\text{Pt}(2,2':4',2''\text{-terpy})\text{Cl}]$.

Figure S18. Cyclic voltammograms of $[\text{Pt}(2,2':4',2''\text{-terpy})(\text{C}\equiv\text{CPh})]$.

Figure S19. UV-vis absorption spectra of the terpyridine ligands in THF.

Figure S20. UV-vis absorption spectra of the $[\text{Pd}(\text{Y-terpy})\text{Cl}]$ complexes in THF.

Figure S21. UV-vis absorption spectra of the $[\text{Pt}(\text{Y-terpy})\text{Cl}]$ complexes in THF.

Figure S22. UV-vis absorption spectra of $[\text{Pt}(\text{Y-terpy})\text{CCPh}]$ complexes in THF.

3. Supplementary Tables

Table S1. Crystal data and structure refinement for $[\text{M}(\text{Y-terpy})\text{X}]$ complexes.

Table S2. Selected bond lengths (Å) and angles (°) for $[\text{M}(\text{Y-terpy})\text{X}]$ complexes.

Table S3. Redox potentials of the complexes $[\text{M}(\text{Y-terpy})\text{X}]$ (M = Pt, Pd, Ni), and related complexes.

Table S4. Selected UV-vis absorption maxima of Y-terpy ligands, $[\text{M}(\text{Y-terpy})\text{X}]$ complexes, and related complexes.

1. Syntheses

1.1 Syntheses of Ligand Precursors

(3-Pyridinyl)-dimethylaminopropen-2-one

4.85 g (4.40 mL, 40.0 mmol, 1.00 eq.) 3-acetylpyridine and 7.15 g (8.00 mL, 60.0 mmol, 1.50 eq.) dimethylformamide-dimethoxyacetal (DMF-DMA) were added to a round bottom flask with 50 mL of *p*-xylene. The mixture was heated under reflux for 19 h from a mixture of AcOEt and *c*-hexane to yield 5.43 g (25.6 mmol, 64%) yellow crystals. ¹H NMR: (CDCl₃, 300 MHz) δ [ppm] = 9.09 (d, ³J = 2.0 Hz, 1H), 8.47 (dd, ³J = 4.8 Hz, ⁴J = 1.8 Hz, 1H), 8.19 (dt, ³J = 7.8 Hz, ⁴J = 2.0 Hz, 1H), 7.84 (d, ³J = 12.2 Hz, 1H), 7.35 (dd, ³J = 7.9 Hz, ⁴J = 4.8 Hz, 1H), 5.68 (d, ³J = 12.3 Hz, 1H), 3.18 (s, 3H), 2.95 (s, 3H).

(4-Pyridinyl)-dimethylaminopropen-2-one

4-Acetylpyridine (1.36 g, 1.50 mL, 11.2 mmol, 1.00 eq.) and dimethylformamide-dimethoxyacetal (DMF-DMA) (2.67 g, 2.98 mL, 22.4 mmol, 2.00 eq.) were added to a microwave vial and heated to 120 °C at constant power (300 W) for 3 minutes. After cooling to room temperature, the formed yellow crystals were filtered off and recrystallised from a mixture of AcOEt and *c*-hexane to yield the desired product as yellow crystals (1.49 g, 8.45 mmol, 75%). ¹H NMR: (CDCl₃, 300 MHz) δ [ppm] = 8.70 (d, ³J = 5.7 Hz, 2H, H1), 7.85 (d, ³J = 12.3 Hz, 1H), 7.68 (d, ³J = 5.6 Hz, 2H), 5.65 (d, ³J = 12.3 Hz, 1H), 3.19 (s, 3H), 2.96 (s, 3H).

1.2 Syntheses of Terpy Ligands

2,2':6',3''-Terpyridine

Under argon atmosphere 7.18 g (64.0 mmol, 2.50 eq.) of KO^tBu were suspended in freshly distilled THF. 3.10 g (2.87 mL, 25.6 mmol, 1.00 eq.) of 2-acetylpyridine were added and the mixture stirred for 2 hours at room temperature, giving a pale-yellow suspension. 5.43 g (25.6 mmol, 1.00 eq.) of (3-pyridinyl)-dimethylaminopropen-2-one were added along with an additional 50 mL of THF, giving a dark red suspension. The mixture was stirred at room temperature for 18 h. 19.7 g (256 mmol, 10.0 eq.) of NH₄OAc were dissolved in 100 mL of HOAc were added and the mixture was heated under reflux for 22 hours. The solvent volume was reduced to half before the mixture was neutralised with aq. Na₂CO₃. The brown oil was extracted with 3x100 mL CHCl₃ and the solvent evaporated. The crude product was purified by column chromatography (SiO₂, *c*-hexane/acetone 1:1, R_f = 0.42) to yield 1.11 g (4.75 mmol, 19%) of a colourless powder. ¹H NMR: (CDCl₃, 300 MHz) δ [ppm] = 9.36 (s, 1H, H1), 8.76-8.66 (m, 2H, H15, H2), 8.61 (d, ³J = 8.0 Hz, 1H, H9), 8.49-8.39 (m, 2H, H4, H12), 7.98-7.75 (m, 3H, H8, H13, H7), 7.44 (dd, ³J = 8.1 Hz, ⁴J = 4.8 Hz, 1H, H3), 7.35 (dd, ³J = 7.6 Hz, ⁴J = 4.8 Hz, 1H, H14). ¹³C NMR: (CDCl₃, 75 MHz) δ [ppm] = 156.2 (C10), 155.3 (C11), 153.6 (C6), 150.0 (C1, C2), 149.1 (C15), 137.9 (C8), 136.8 (C13), 135.4 (C3), 123.8 (C14), 121.1 (C4, C12), 121.0 (C7, C9). HR-ESI-MS (70 eV): m/z = 234.10 [M+H⁺], 256.08 [M+Na⁺].

2,2':6',4''-Terpyridine

Under argon atmosphere 3.85 g (34.3 mmol, 2.5 eq.) of KO^tBu were suspended in 60.0 mL of distilled THF. After 15 minutes of stirring at room temperature, 1.66 g (1.54 mL, 14.2 mmol, 1.00 eq.) 2-acetylpyridine was added and further stirred. The colourless cloudy suspension turned yellow. After 2 hours, 2.90 g (13.7 mmol, 1.00 eq.) of 3-(dimethylamino)-1-(pyridin-4-yl)prop-2-en-1-one were added, leading to an immediate change of colour to deep red. The mixture was stirred at room temperature for 26 hours before 10.6 g (137 mmol, 10.0 eq.) of NH₄OAc was added along with 35.0 mL of acetic acid. The mixture was heated to reflux for 17 hours, leading to a colour change to dark brown. After cooling to room temperature, the solvent volume was reduced to half. The remaining acid was neutralised using Na₂CO₃ and the crude mixture poured into a mixture of 200 mL distilled water and 200 mL CHCl₃. The organic phase was washed three times with 100 mL of distilled water and dried over MgSO₄. The solvent was evaporated, leaving brown oil. The crude product was purified *via* column chromatography (SiO₂, *c*-hexane/acetone 2:1, R_f = 0.28) to yield 1.04 g (4.40 mmol, 32%) as a beige powder. ¹H NMR: (CDCl₃, 300 MHz) δ [ppm] = 8.76 (d, ³J = 6.2 Hz, 2H, H1, H1'), 8.71 (ddd, ³J = 4.7 Hz, ⁴J = 1.8 Hz, ⁵J = 1.0 Hz, 1H, H13), 8.61 (d, ³J = 7.9 Hz, 1H, H10), 8.49 (dd, ³J = 7.9 Hz, ⁴J = 1.1 Hz, 1H, H7), 8.03 (d, ³J = 6.1 Hz, 2H, H2, H2'), 7.94 (t, ³J = 7.8 Hz, 1H, H6), 7.87 (td, ³J = 7.7 Hz, ⁴J = 1.8 Hz, 1H, H11), 7.83 (dd, ³J = 7.8, ⁴J = 1.1 Hz, 1H),

7.35 (ddd, $^3J = 7.5$ Hz, $^3J = 4.8$ Hz, $^4J = 1.3$ Hz, 1H, H12), ^{13}C NMR: (CDCl_3 , 75 MHz) δ [ppm] = 156.2 (C8), 155.9 (C9), 153.6 (C4), 150.5 (C1, C1'), 149.2 (C13), 146.3 (C3), 138.0 (C6), 137.0 (C11), 124.0 (C12), 121.3 (C10), 121.1 (C2, C2'), 120.6 (C5, C7). HR-ESI-MS (70 eV): $m/z = 234.10$ [$\text{M}+\text{H}^+$], 256.08 [$\text{M}+\text{Na}^+$].

2,2':4',2''-Terpyridine

14.2 mL (35.5 mmol, 3.20 eq) of *n*-BuLi (2.5 M in *n*-hexane) was dissolved in 70.0 mL of distilled THF and reacted slowly with 3.17 mL (5.26 g, 33.3 mmol, 3.00 eq.) of 2-bromopyridine dissolved in 10.0 mL of THF for 30 minutes at -78 °C. 5.45 g (40.0 mmol, 3.60 eq.) of dried ZnCl_2 were suspended in 30.0 mL of THF and added to the reaction, which was warmed up to room temperature. 641 mg (555 μmol , 5 mol%) of the catalyst $[\text{Pd}(\text{PPh}_3)_4]$ and 2.63 g (11.1 mmol, 1.00 eq.) of 2,4-dibromopyridine were added and the mixture heated under reflux for 19 hours. The mixture was quenched with aq. NH_4Cl solution and extracted with AcOEt and CHCl_3 . The combined organic phases were evaporated to yield 493 mg (2.11 mmol, 19%) of a colourless solid. ^1H NMR: (CDCl_3 , 500 MHz) δ [ppm] = 8.98 (d, $^4J = 2.3$ Hz, 1H, H10), 8.80 (d, $^3J = 5.2$ Hz, 1H, H8), 8.76 (d, $^3J = 4.7$ Hz, 1H, H15), 8.72 (d, $^3J = 4.3$ Hz, 1H, H1), 8.46 (d, $^3J = 7.9$ Hz, 1H, H4), 8.01 (dd, $^3J = 5.0$ Hz, $^4J = 1.8$ Hz, 1H, H7), 7.97 (d, $^3J = 7.9$ Hz, 1H, H12), 7.83 (qd, $^3J = 7.9$ Hz, $^4J = 1.8$ Hz, 2H, H13, H3), 7.33 (dtd, $^3J = 7.5$ Hz, $^3J = 4.8$ Hz, $^4J = 1.2$ Hz, 2H, H14, H2). ^{13}C NMR: (CDCl_3 , 75 MHz) δ [ppm] = 156.8 (C5), 156.1 (C11), 154.8 (C6), 150.0 (C15), 149.9 (C8), 149.2 (C1), 147.5 (C9), 136.9 (C3, C13), 123.8 (C14), 123.7 (C2), 121.2 (C4, C12), 121.1 (C7), 118.4 (C10). HR-ESI-MS (70 eV): $m/z = 234.01$ [$\text{M}+\text{H}^+$], 256.08 [$\text{M}+\text{Na}^+$].

2,3':5',2''-Terpyridine

25.4 mL (64.0 mmol, 3.20 eq) of *n*-BuLi (2.5 M in *n*-hexane) was dissolved in 140 mL of distilled THF and reacted slowly with 5.95 mL (9.48 g, 60.0 mmol, 3.00 eq.) of 2-bromopyridine dissolved in 20.0 mL of THF for 30 min at -78 °C. 10.9 g (80.0 mmol, 4.00 eq.) of dried ZnCl_2 were suspended in 60.0 mL of THF and added to the reaction mixture, which was warmed up to room temperature. 1.16 g (1.00 mmol, 5 mol%) of the catalyst $[\text{Pd}(\text{PPh}_3)_4]$ and 4.74 g (20.0 mmol, 1.00 eq.) of 3,5-dibromopyridine were added and the mixture heated under reflux for 16 hours. The product was obtained as a colourless solid (3.31 g, 14.2 mmol, 71%). $R_f = 0.2$ (SiO_2 , AcOEt/ *c*-hexane 1:1 v/v). Elemental analysis found (calculated for $\text{C}_{15}\text{H}_{11}\text{N}_3$, $M = 233.27$ g mol^{-1}): C, 77.23 (76.76); H, 4.75 (5.01); N, 18.01 (16.79). ^1H NMR: (CDCl_3 , 300 MHz) δ [ppm] = 9.34 (d, $^4J = 2.2$ Hz, 2H, H5), 9.09 (t, $^4J = 2.2$ Hz, 1H, H6), 8.77 (d, $^3J = 4.8$ Hz, 2H, H1), 8.20 (d, $^3J = 7.9$ Hz, 2H, H4), 7.98 (td, $^3J = 7.7$ Hz, $^4J = 1.8$ Hz, 2H, H3), 7.47 (dd, $^3J = 7.0$ Hz, $^3J = 5.4$ Hz, 2H, H2). ^{13}C NMR: (CDCl_3 , 75 MHz) δ [ppm] = 154.0 (C8), 150.4 (C1), 148.4 (C5), 138.0 (C3), 134.5 (C7), 132.1 (C6), 123.9 (C2), 121.4 (C4). EI-MS (70 eV): $m/z = 234.1$ [$\text{M}+\text{H}^+$].

2. Supplementary Figures

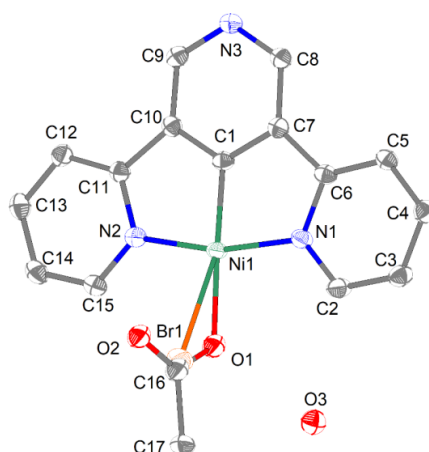


Figure S1. Molecular structure of $[\text{Ni}(2,3':5',2''\text{-terpy})\text{Br}_{0.14}/\text{OAc}_{0.86}]\cdot\text{H}_2\text{O}$ from single crystal X-ray diffraction ORTEP plot with displacement ellipsoids at 50% probability. H atoms were omitted for clarity.

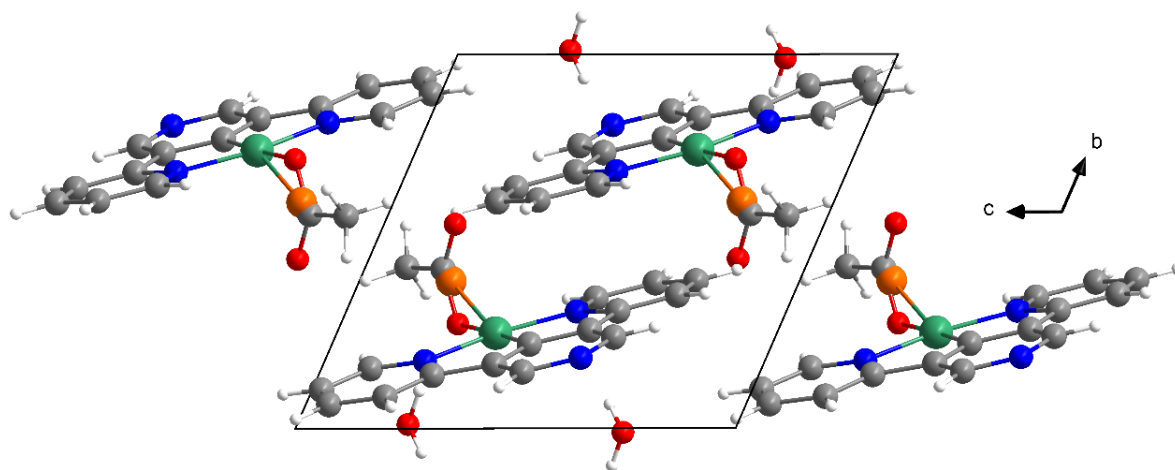


Figure S2. View on the crystal structure of $[\text{Ni}(2,3':5',2''\text{-terpy})\text{Br}_{0.14}/\text{OAc}_{0.86}]\cdot\text{H}_2\text{O}$ along the crystallographic a -axis.

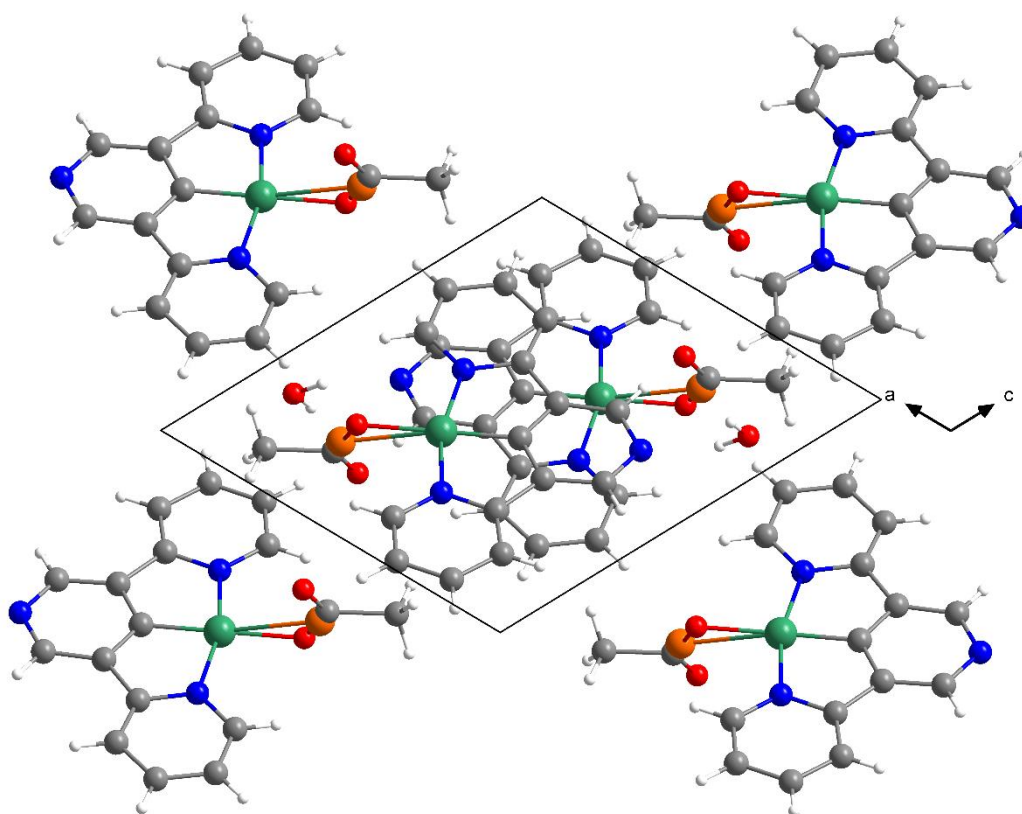


Figure S3. View on the crystal structure of $[\text{Ni}(2,3':5',2''\text{-terpy})\text{Br}_{0.14}/\text{acetate}_{0.86}]\cdot\text{H}_2\text{O}$ along the crystallographic b -axis.

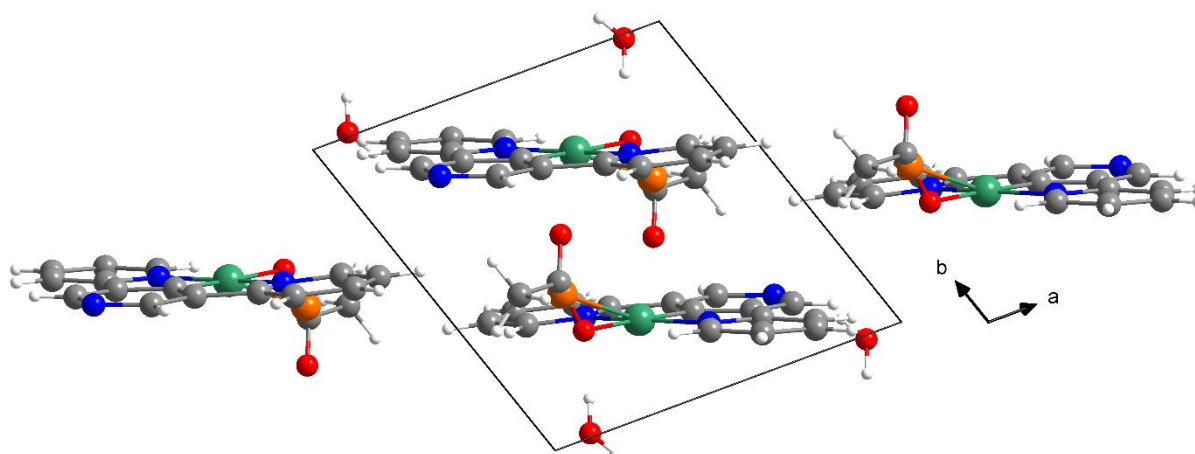


Figure S4. View on the crystal structure of $[\text{Ni}(2,3':5',2''\text{-terpy})\text{Br}_{0.14}/\text{acetate}_{0.86}]\cdot\text{H}_2\text{O}$ along the crystallographic c -axis.

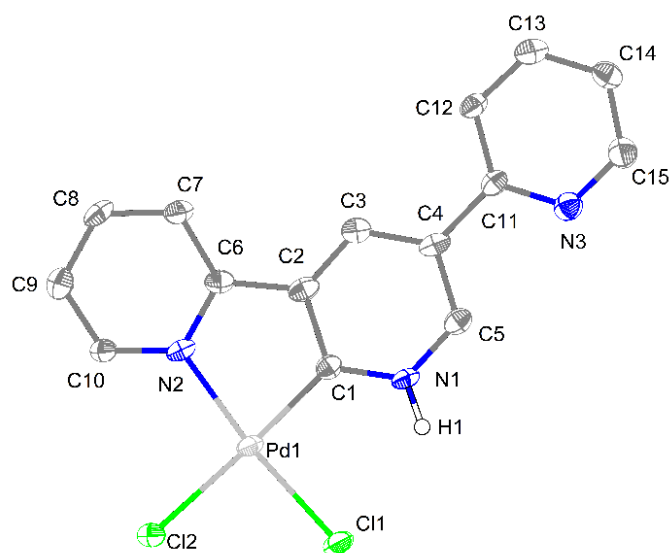


Figure S5. Molecular structure of $[\text{Pd}(2,3':5',2''\text{-terpyH})\text{Cl}_2]$ from single crystal X-ray diffraction (ORTEP plot with displacement ellipsoids at 50% probability). H atoms were omitted for clarity.

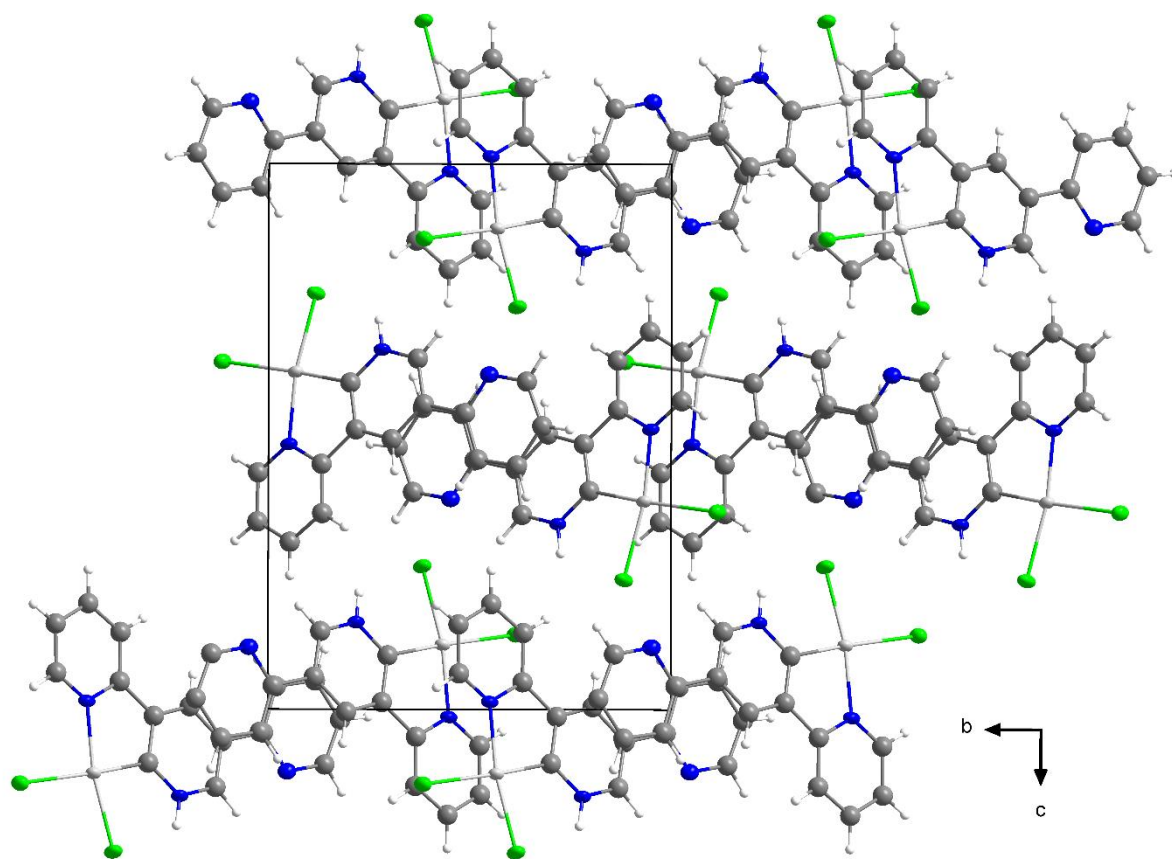


Figure S6. View on the crystal structure of $[\text{Pd}(2,3':5',2''\text{-terpyH})\text{Cl}_2]$ along the crystallographic a -axis.

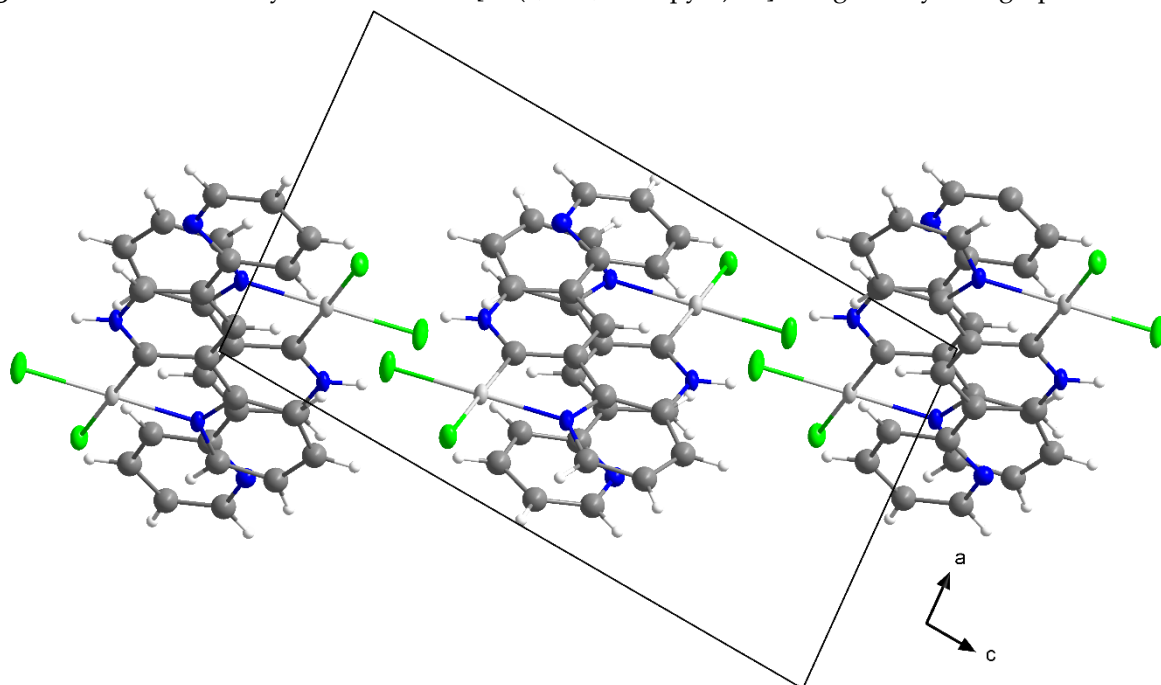


Figure S7. View on the crystal structure of $[\text{Pd}(2,3':5',2''\text{-terpyH})\text{Cl}_2]$ along the crystallographic b -axis.

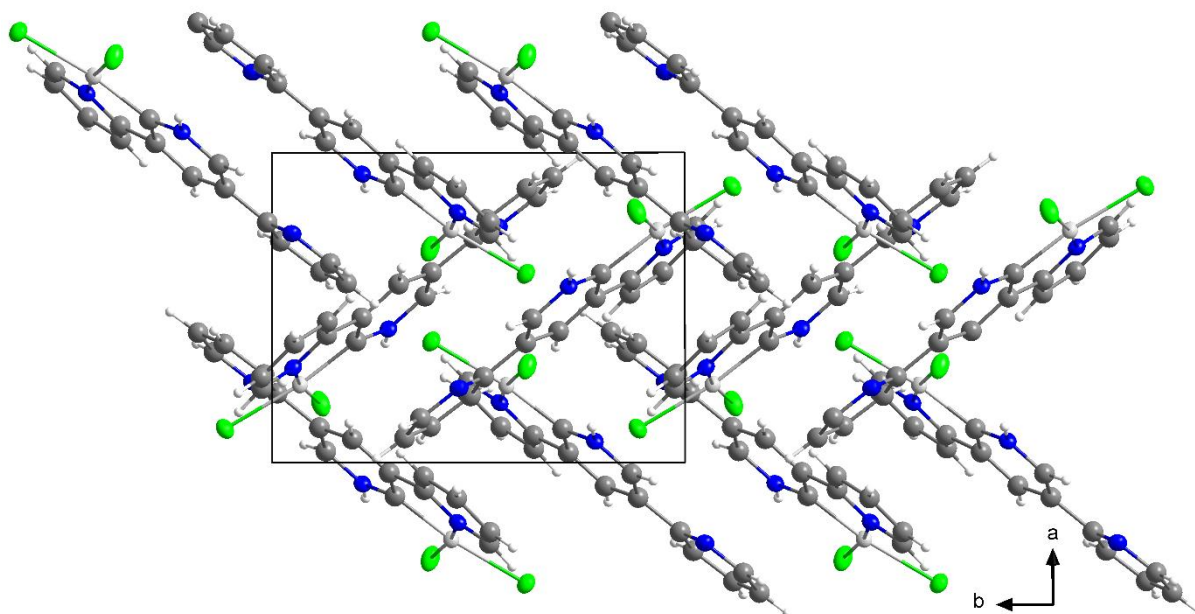


Figure S8. View on the crystal structure $[\text{Pd}(2,3':5',2''\text{-terpyH})\text{Cl}_2]$ along the crystallographic c -axis.

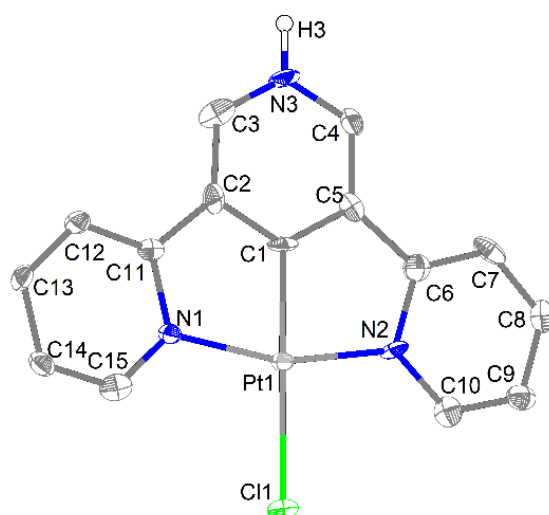


Figure S9. Molecular structure of $[\text{Pt}(2,3':5',2''\text{-terpyH})\text{Cl}]\text{Cl}$ from single crystal X-ray diffraction (ORTEP plot with displacement ellipsoids at 50% probability). H atoms other than the N–H and the Cl⁻ counterion were omitted for clarity

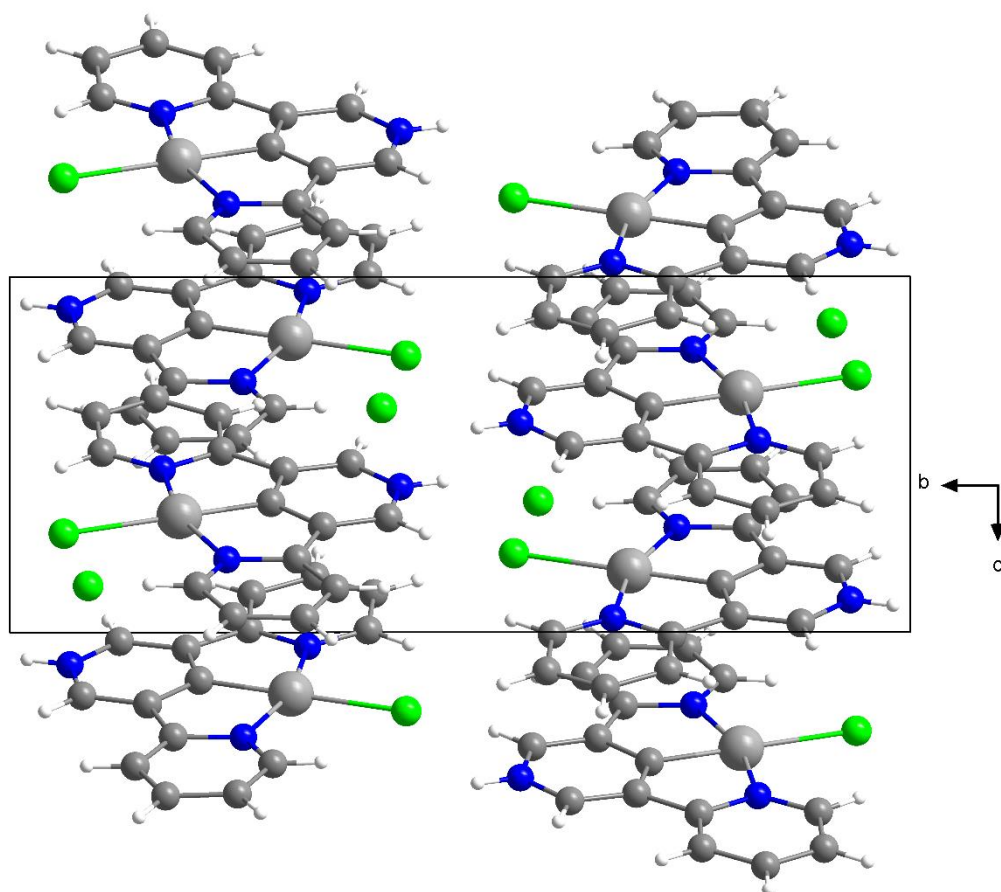


Figure S10. View on the crystal structure of $[\text{Pt}(2,3':5',2''\text{-terpyH})\text{Cl}]\cdot\text{Cl}$ along the crystallographic a -axis.

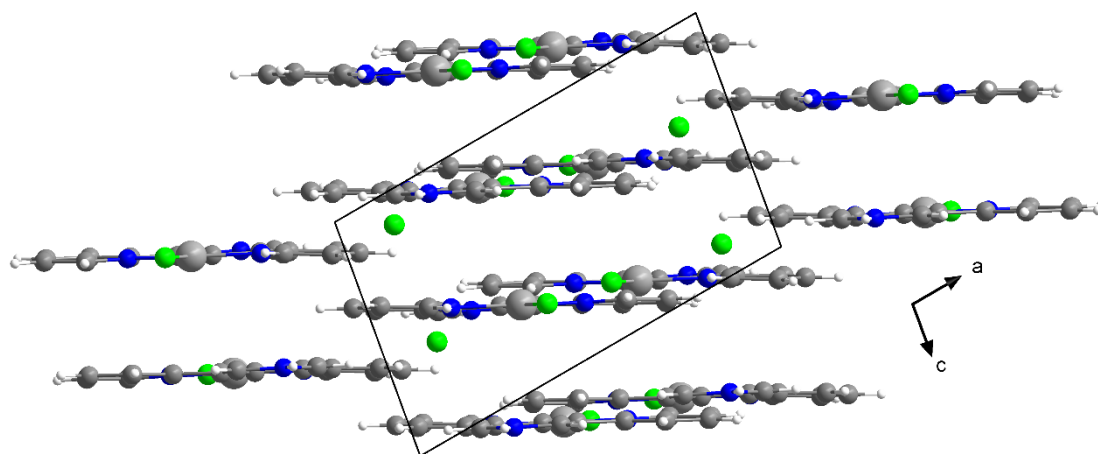


Figure S11. View on the crystal structure of $[\text{Pt}(2,3':5',2''\text{-terpyH})\text{Cl}]\cdot\text{Cl}$ along the crystallographic b -axis.

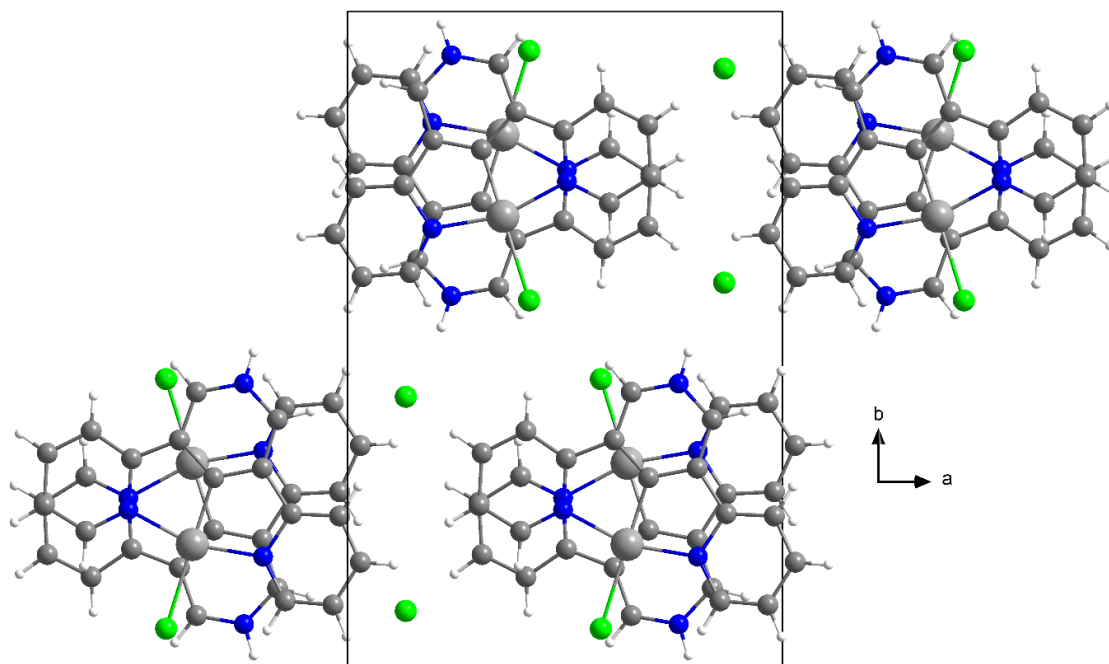


Figure S12. View on the crystal structure of $[\text{Pt}(2,3':5',2''\text{-terpyH})\text{Cl}]\cdot\text{Cl}$ along the crystallographic c -axis.

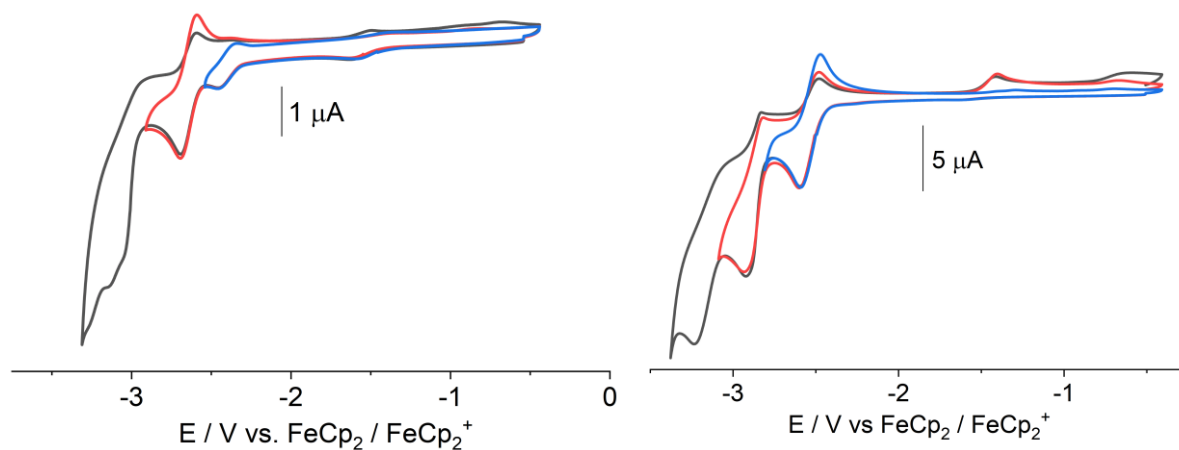


Figure S13. Cyclic voltammograms of 2,2':6',3''-terpy (left) and 2,2':6',4''-terpy (right), in 0.1 M $n\text{-Bu}_4\text{NPF}_6$ solution in THF at room temperature at a scan rate of 100 mV/s.

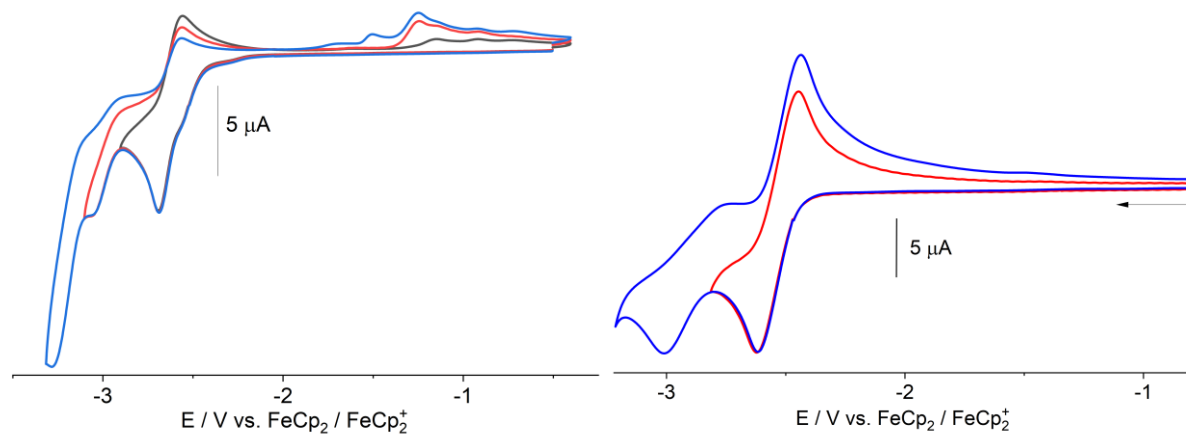


Figure S14. Cyclic voltammograms of 2,3':5',2''-terpy (left) and 2,2':4',2''-terpy (right), in 0.1 M $n\text{-Bu}_4\text{NPF}_6$ solution in THF at room temperature at a scan rate of 100 mV/s.

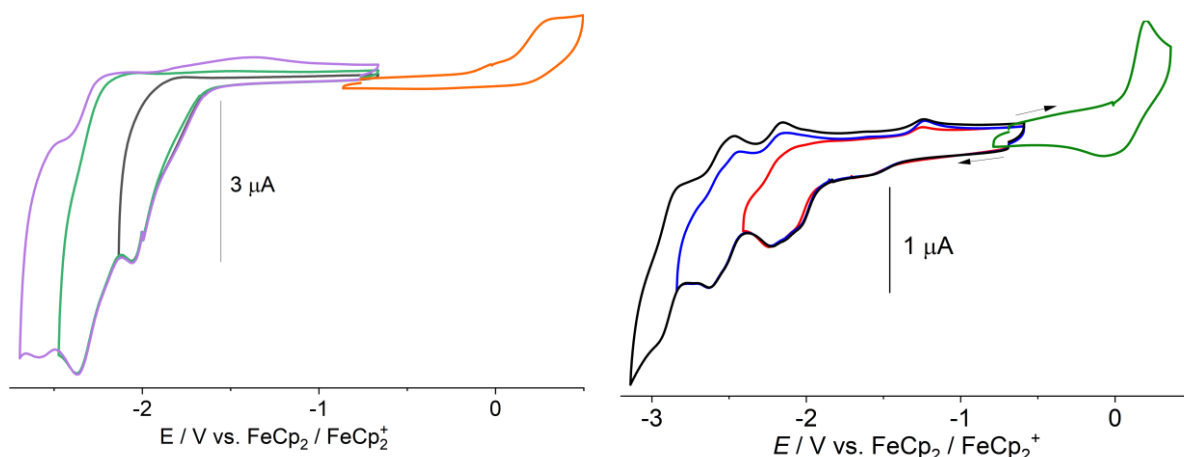


Figure S15. Cyclic voltammograms of [Ni(2,3':5',2''-terpy)Br] (left) and [Ni(2,2':4',2''-terpy)Br] (right) in 0.1 M *n*-Bu₄NPF₆ solution in THF at room temperature at a scan rate of 100 mV/s.

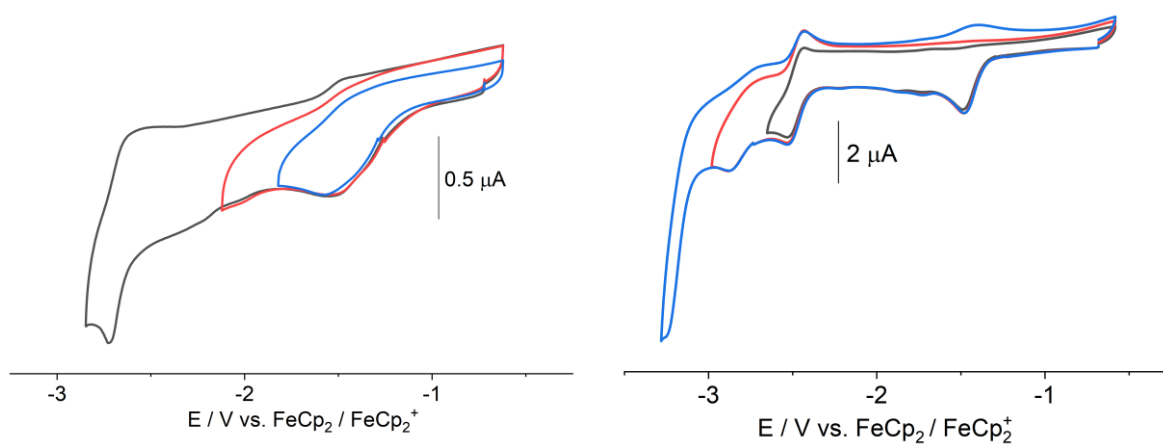


Figure S16. Cyclic voltammograms of [Pd(2,3':5',2''-terpy)Cl] (left) and [Pd(2,2':4',2''-terpy)Cl] (right), in 0.1 M *n*-Bu₄NPF₆ solution in THF at room temperature at a scan rate of 100 mV/s.

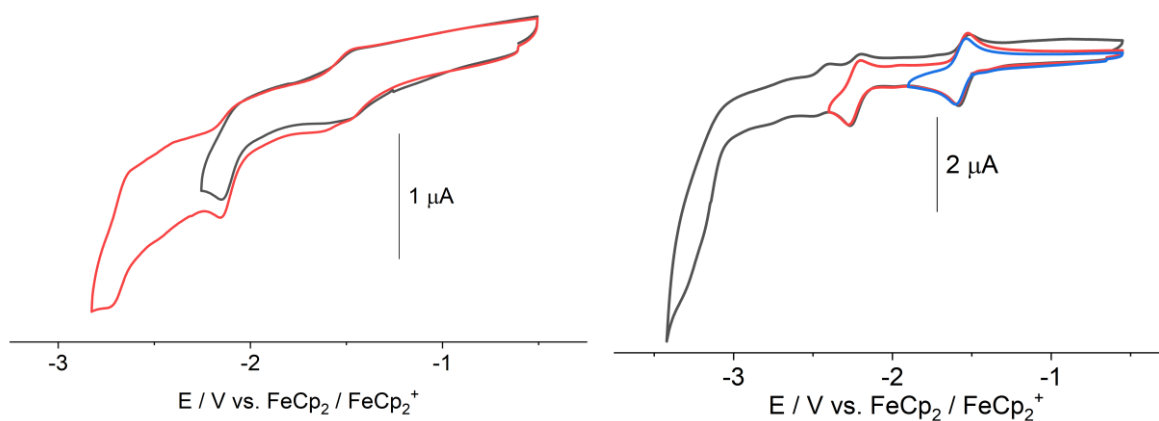


Figure S17. Cyclic voltammograms of [Pt(2,3':5',2''-terpy)Cl] (left) and [Pt(2,2':4',2''-terpy)Cl] (right), in 0.1 M *n*-Bu₄NPF₆ solution in THF at room temperature at a scan rate of 100 mV/s.

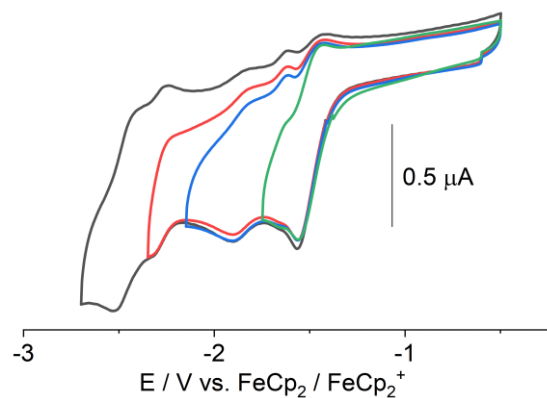


Figure S18. Cyclic voltammograms of $[\text{Pt}(2,2':4',2''\text{-terpy})(\text{C}\equiv\text{CPh})]$ in 0.1 M $n\text{-Bu}_4\text{NPF}_6$ solution in THF at room temperature at a scan rate of 100 mV/s.

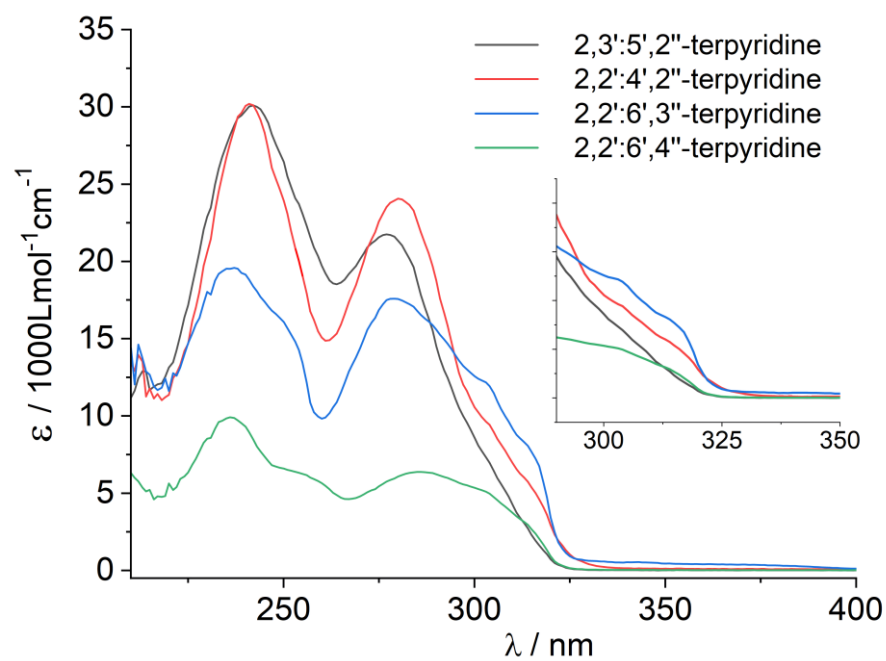


Figure S19. UV-vis absorption spectra of the terpyridine ligands in THF at room temperature.

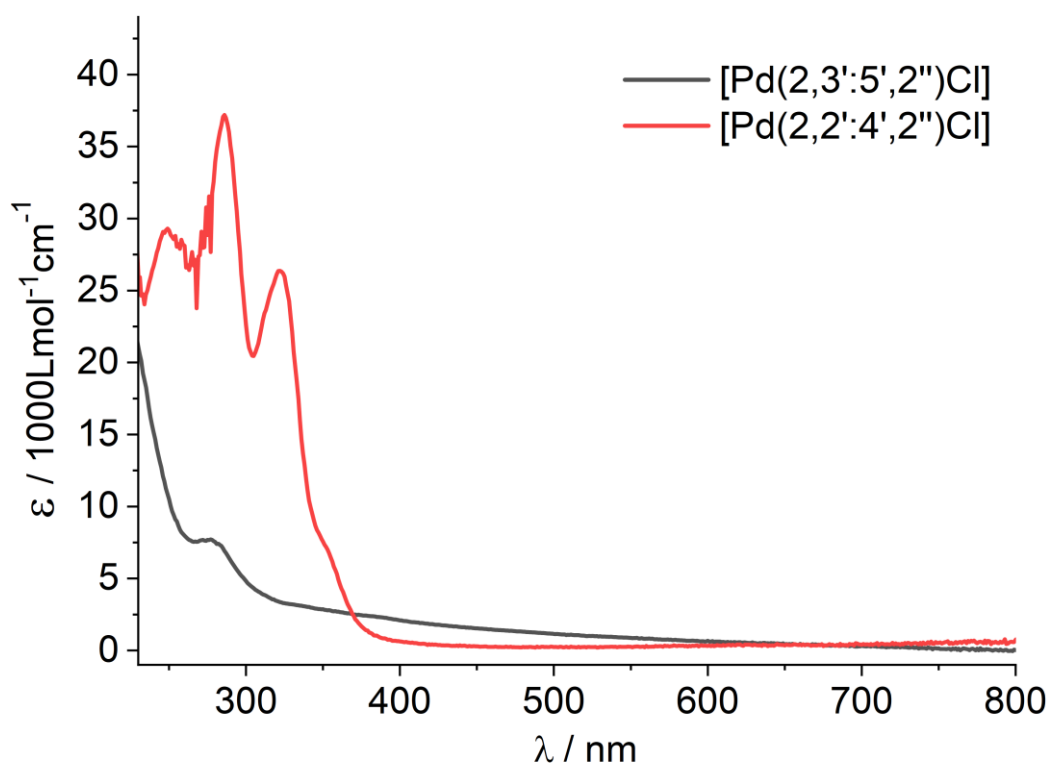


Figure S20. UV-vis absorption spectra of the [Pd(Y-terpy)Cl] complexes, measured in THF at room temperature.

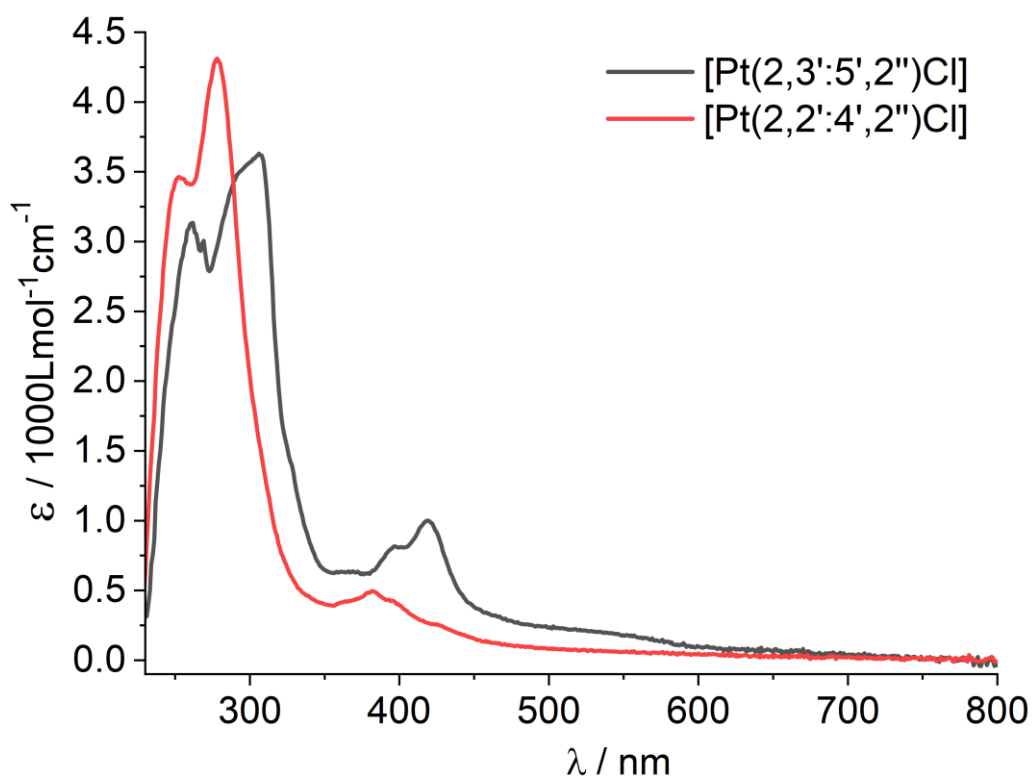


Figure S21. UV-vis absorption spectra of the [Pt(Y-terpy)Cl] complexes measured in THF at room temperature.

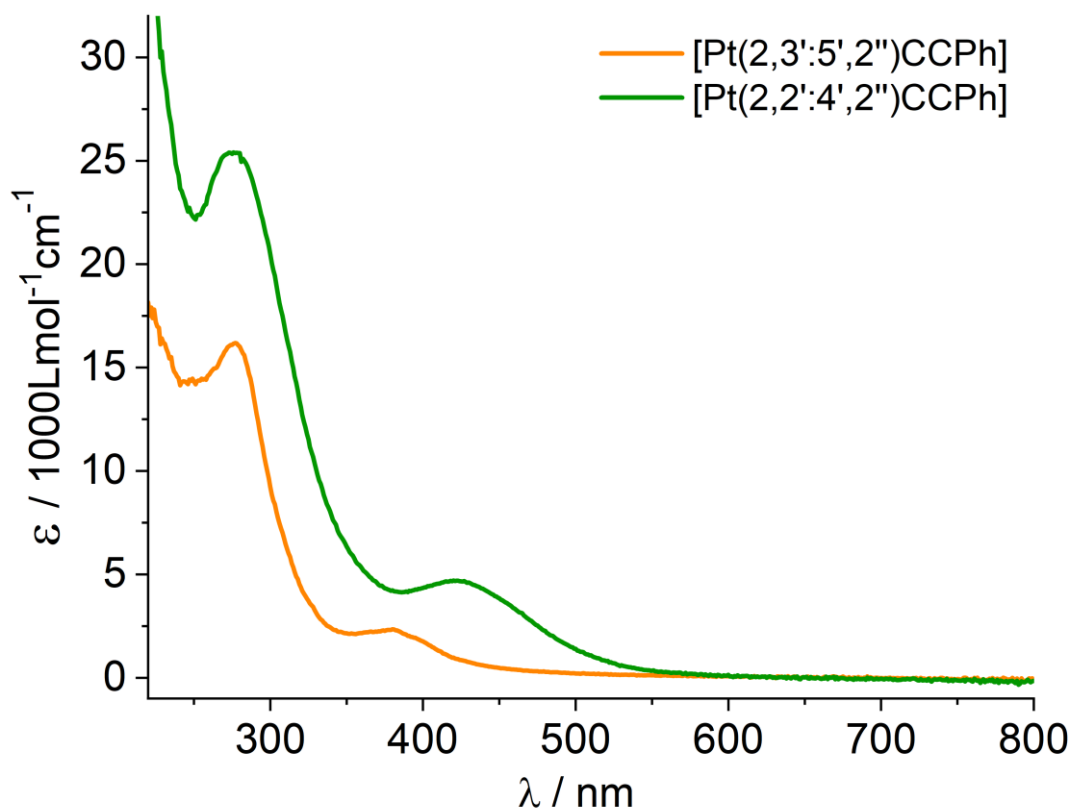


Figure S22. UV-vis absorption spectra of [Pt(Y-terpy)CCPh] complexes measured in THF at room temperature.

3. Supporting Tables

Table S1. Crystal data and structure refinement for [M(Y-terpy)X] complexes.

	[Ni(2,3':5',2''-terpy)Br _{0.13} /OAc _{0.87}].H ₂ O	[Pd(2,3':5',2''-terpyH)Cl ₂]	[Pt(2,3':5',2''-terpyH)Cl]Cl
CCDC	2250815	2250813	2250812
Empirical formula	C _{16.75} H _{14.16} Br _{0.13} N ₃ NiO _{2.75}	C ₁₅ H ₁₁ Cl ₂ N ₃ Pd	C ₁₅ H ₁₁ Cl ₂ N ₃ Pt
Formula weight /g mol ⁻¹	370.43	410.57	499.26
Temperature /K	100.00	100	100
wavelength /Å	0.71073	0.71073	0.71073
Crystal System	triclinic	monoclinic	monoclinic
Space Group	P $\bar{1}$	P2 ₁ /n	P2 ₁ /c
Unit Cell			
a /Å	9.0873(2)	8.4780(7)	11.8804(7)
b /Å	9.1759(2)	11.2429(8)	17.6631(2)
c /Å	10.6324(3)	15.3079(1)	7.0849(5)
α /°	107.512(1)	90	90
β /°	113.001(1)	95.662(2)	99.996(2)
γ /°	99.244(1)	90	90
Volume /Å ³	738.14(3)	1452.01(2)	1464.16(7)
Z	2	4	4
ρ_{calc} /Mg/m ³	1.667	1.878	2.265
μ /mm ⁻¹	1.685	1.640	9.943
F (000)	380.0	808.0	936.0

Crystal size /mm ³	0.09 × 0.03 × 0.01	0.07 × 0.05 × 0.03	0.09 × 0.02 × 0.01
θ range for data collect. /°	4.542 to 52.832	4.502 to 52.744	4.176 to 51.36
Index ranges	-11 ≤ h ≤ 11	-10 ≤ h ≤ 10	-14 ≤ h ≤ 13
	-11 ≤ k ≤ 11	-14 ≤ k ≤ 14	-21 ≤ k ≤ 21
	-13 ≤ l ≤ 13	-18 ≤ l ≤ 18	-8 ≤ l ≤ 8
Reflections coll. / Independ.	45410 / 3018	12605 / 2939	24767 / 2788
R _{int}	0.0309	0.0690	0.1166
Completeness to θ = 26.42 °	0.992	0.992	0.999
Absorption correction	Multi-Scan	Multi-Scan	Multi-Scan
Max. and min. transmission	0.745, 0.501	0.746, 0.613	0.746, 0.515
Data/ restraints/ param.	3018 / 0 / 223	2939/0/194	2788 / 0 / 191
GOOF on F ²	1.210	1.026	1.035
Final R indices [I>2σ(I)] ^a	R ₁ = 0.0319, wR ₂ = 0.069	R ₁ = 0.0423, wR ₂ = 0.0911	R ₁ = 0.0383, wR ₂ = 0.0739
R indices (all data)	R ₁ = 0.0327, wR ₂ = 0.0693	R ₁ = 0.0668, wR ₂ = 0.1019	R ₁ = 0.0583, wR ₂ = 0.0847
Larg. diff. peak&hole /e·Å ⁻³	0.54 / -0.46	0.79/ -0.89	1.35 / -1.42

$$^a R_1 = \frac{\sum ||F_o| - |F_c||}{\sum |F_o|}; wR_2 = \left[\frac{\sum [w(F_o^2 - F_c^2)^2]}{\sum [w(F_o^2)^2]} \right]^{1/2}$$

Table S2. Selected bond lengths (Å) and angles (°) for [M(Y-terpy)X] complexes.

[Ni(2,3':5',2''-terpy)Br _{0.13} /OAc _{0.87}]·H ₂ O		[Pd(2,3':5',2''-terpyH)Cl ₂]		[Pt(2,3':5',2''-terpyH)Cl]·Cl	
Distances / Å		Distances / Å		Distances / Å	
Ni1–C7	1.805(2)	Pd1–C1	1.943(5)	Pt1–C1	1.896(8)
Ni1–N1	1.923(2)	-	-	Pt1–N1	2.039(8)
Ni1–N2	1.923(2)	Pd1–N2	2.042(4)	Pt1–N2	2.025(8)
Ni1–O1	2.962(3)	-	-	-	-
Ni1–O2	1.929(2)	Pd1–Cl1	2.285(1)	N3H–Cl2	2.181(3)
Ni1–Br1	2.487(8)	Pd1–Cl2	2.377(1)	Pt1–Cl1	2.382(2)
Angles / °		Angles / °		Angles / °	
C7–Ni1–N1	82.37(9)	C1–Pd1–N2	80.90(2)	C1–Pt1–N1	81.2(4)
C7–Ni1–N2	82.24(9)	C1–Pd1–Cl1	91.83(2)	C1–Pt1–N2	80.9(4)
N1–Ni1–O2	99.28(8)	Cl1–Pd1–Cl2	91.80(5)	N1–Pt1–Cl1	99.1(2)
N2–Ni1–O2	96.05(8)	Cl2–Pd1–N2	96.05(2)	N2–Pt1–Cl1	98.8(2)
N1–Ni1–Br1	93.49(2)	-	-	-	-
N2–Ni1–Br1	101.08(2)	-	-	-	-
N1–Ni1–N2	164.43(8)	C1–Pd1–Cl2	172.68(2)	N1–Pt1–N2	162.1(3)
C7–Ni1–Br1	160.03(2)	N2–Pd1–Cl1	170.84(2)	C1–Pt1–Cl1	179.6(3)
C7–Ni1–O2	177.86(10)	-	-	-	-
Sum / ° ^a	359.94(2)		360.00		360.00
π-stacking / Å ^b					
3.6702(1)		3.6338(1)		3.7405(1)	

^a Sum of angles around the central metal atom. ^b Shortest centroid...centroid distance.

Table S3. Redox potentials of the complexes [M(Y-terpy)X] (M = Pt, Pd, Ni), and related complexes.^a

[M(Y-terpy)X]	E (red2)	E (red1)	E (ox1)	ΔE (red1-red2)	ΔE_{redox} (ox1-red1)
Ligands					
2,3':5',2''	-3.07	-2.63	-	0.44	-
2,2':4',2''	-3.00	-2.51	-	0.49	-
M = Ni, X = Br					
2,3':5',2''	-2.37	-2.06	0.31	0.31	2.37 ^e
2,2':4',2''	-2.62	-2.22	0.21	0.40	2.43 ^e
[Ni(dpb)Br] ^b	-2.75	-2.30	0.07	0.45	2.37
[Ni(dpb)Cl] ^b	-2.57	-2.33	0.06	0.24	2.39
M = Pd, X = Cl					
2,3':5',2''	-2.01	-1.58	-	0.43	3.13 ^e
2,2':4',2''	-2.50	-1.49	-	1.01	3.04 ^e
[Pd(Me ₂ dpb)Cl] ^c	-2.75	-2.34	0.74	0.41	3.08
M = Pt, X = Cl					
2,3':5',2''	-2.16	-1.47	-	0.69	3.02 ^e
2,2':4',2''	-2.24	-1.55	-	0.69	3.10 ^e
[Pt(dpb)Cl] ^d	-2.60	-2.17	0.41	0.43	2.58

^aFrom cyclic voltammetry in *n*Bu₄NPF₆/THF (tetrahydrofuran). Potentials in V vs. ferrocene/ferrocenium; accuracy of potentials: ± 0.003 V. ^bFrom ref. 1. ^cFrom ref. 2. ^dFrom ref. 3. ^e ΔE = THF discharge limit - Red1.

Table S4. Selected UV-vis absorption maxima of Y-terpy ligands, [M(Y-terpy)X] complexes, and related complexes.^a

[M(Y-terpy)X]	λ_1 (ε)	λ_2 (ε)	λ_3 (ε)	λ_4 (ε)	λ_5 (ε)	λ_6 (ε)
Y-terpy ligands						
Y = 2,3':5',2''	242(30)	277(22)				
Y = 2,2':4',2''	241(30)	280(24)				
M = Ni, X = Br						
Y = 2,3':5',2''	238 (31)	268 (24)	332 (9.3)	-	404 (4.4)	466 (1.7)
Y = 2,2':4',2''	236 (36)	274 (22)	303 (12)	-	398(4.9)	431 (6.4)
[Ni(dpb)Br] ^b	240 (37)	277 (29)	-	336 (5.4)	411 (6.0)	433 (5.6)
M = Pd, X = Cl						
Y = 2,3':5',2''	278 (23)	-	331(9.6)	389(7.8)		
Y = 2,2':4',2''	249 (29)	286 (37)	322 (26)	-	355 (6.6)	
[Pd(Me ₂ dpb)Cl] ^c	239(27)	275(23)	283(22)	327(8.3)	360(7.4)	375(1.2)
M = Pt, X = Cl						
Y = 2,3':5',2''	261 (3.1)	269 (3.0)	291 (3.5)	306 (3.6)	396 (0.8)	419 (0.1)
Y = 2,2':4',2''	252 (3.4)	277 (4.3)	-	-	381 (0.5)	427 (0.4)
[Pt(dpb)Cl] ^d	255 (25)	289 (21)	332 (6.3)	379 (8.6)	402 (7.0)	485 (0.1)
M = Pt, X = C≡CPh						
Y = 2,3':5',2''	277 (16)	381 (2.4)	395(1.9)			
Y = 2,2':4',2''	276 (25)	424 (4.6)				
[Pt(dpb)(C≡CPh)] ^e	265 (45)	291 (35)	378 (8)	391 (9)		

^a Absorption maxima λ in nm in THF solution at rt; molar absorption coefficient ϵ in 1000 L mol⁻¹ cm⁻¹.

^b From ref. 1. ^c From ref. 2 ^d From refs. 3 and 4. ^e From ref. 5.

References

1. Kletsch, L.; Hörner, G.; Klein, A. Cyclometalated Ni(II) complexes [Ni(N[^]C[^]N)X] of the tridentate 2,6-di(2-pyridyl)-phen-ide ligand. *Organometallics* **2020**, *39*, 2820–2829. <https://doi.org/10.1021/acs.organomet.0c00355>
2. Kletsch, L.; Jordan, R.; Köcher, A. S.; Buss, S.; Strassert, C. A.; Klein, A. Photoluminescence of Ni(II), Pd(II), and Pt(II) Complexes [M(Me₂dpb)Cl] Obtained from C–H Activation of 1,5-Di(2-pyridyl)-2,4-dimethylbenzene (Me₂dpbH). *Molecules* **2021**, *26*, 5051. <https://doi.org/10.3390/molecules26165051>
3. Williams, J.A.G; Beeby, A.; Davies, E.S.; Weinstein, J.A.; Wilson, C. An Alternative Route to Highly Luminescent Platinum(II) Complexes: Cyclometalation with N[^]C[^]N-Coordinating Dipyridylbenzene Ligands. *Inorg. Chem.* **2003**, *42*, 8609–8611. <https://doi.org/10.1021/ic035083>
4. Wang, Z.; Turner, E.; Mahoney, V.; Madakuni, S.; Groy, T.; Li, J. Facile Synthesis and Characterization of Phosphorescent Pt(N[^]C[^]N)X Complexes. *Inorg. Chem.* **2010**, *49*, 11276–11286. <https://doi.org/10.1021/ic100740e>
5. Chen, Y.; Li, K.; Lu, W.; Chui, S.S.-Y.; Ma, C.-W; Che, C.-M. Photoresponsive Supramolecular Organometallic Nanosheets Induced by Pt^{II}...Pt^{II} and C–H... π Interactions. *Angew. Chem., Int. Ed.* **2009**, *48*, 9909–9913. <https://doi.org/10.1002/anie.200905678>